Frolich, *Science* **262**, 1525 (1993).
10. E. Rignot, *J. Glaciol.* **42**, 476 (1996).
11. To locate the grounding line with ERS radar interferometry, we used two interferograms formed by combining ERS image data acquired 1 day apart. A DEM was registered to each interferogram from a knowledge of the radar imaging geometry and the satellite precision orbits. The phase variations associated with surface topography and the interferometric baseline were then automatically removed from the interferograms, leaving only phase variations caused by the glacier deformation over 1 day. This deformation is the combination of a long-term motion under the driving stress procured by gravity, and a short-term vertical motion induced by tidal forcing from the ocean. If the glacier velocity (or gravity term) is continuous and steady throughout the period of observation, the differencing of two such interferograms produces a third interferogram which only contains the tidal signal. It is then possible to locate the limit of tidal flexing, or glacier hinge line, within less than 100 m, across the entire glacier width (*10*).
12. L. Koch, *Medd. Groenl.* **65**, 181 (1928).
13. S. Ekholm, *J. Geophys. Res.* **101**, 21961 (1996).
14. An accurate measurement of the ice thickness from the glacier surface elevation requires a knowledge of the density profile with depth. We assumed that the mean glacier ice density, ρ_i, is 917 kg/m^3 for the relatively warm ice of the coastal regions [P. V. Hobbs, *Ice Physics* (Oxford Univ. Press, London, 1974)], and the sea water density, ρ_w, is 1030 kg/m^3 [A. Foldvik, T. Gammelsrød, T. Tørresen, *Polar Res.* **3**, 209 (1985)]. Ice thickness is obtained by multiplying the surface elevation by $\rho_w/(\rho_w-\rho_i)$, or 9.115.
15. T. S. Chuah, S. P. Gogineni, C. Allen, B. Wohletz, *Radar Systems and Remote Sensing Laboratory Technical Report 10470* (University of Kansas, Lawrence, KS, 1996).
16. W. B. Krabill, R. H. Thomas, C. F. Martin, R. N. Swift, E. B. Frederick, *Int. J. Remote Sens.* **16**, 1211 (1995).
17. T. J. O. Sanderson and C. S. M. Doake, *J. Glaciol.* **22**, 285 (1979).
18. Ice flow direction is known within 5°. The line-of-sight interferometric velocity is known within 2 mm/day or 1 m/year. The ERS data had a line-of-sight vector within 30° of the main flow direction.
19. W. S. B. Paterson, *The Physics of Glaciers* (Elsevier Science, Tarrytown, NY, 1994).
20. C. E. Bøggild, N. Reeh, H. Oerter, *Global Planet. Change* **9**, 79 (1994); T. Konzelmann and R. Braithwaite, *J. Glaciol.* **41**, 174 (1995); T. Høy, *Medd. Groenl.* **182**, 1 (1970).
21. S. S. Jacobs, H. H. Helmer, C. S. M. Doake, A. Jenkins, R. M. Frolich, *J. Glaciol.* **38**, 375 (1992); A. Jenkins and C. S. M. Doake, *J. Geophys. Res.* **96**, 791 (1991); D. R. McAyeal, *ibid.* **89**, 597 (1984).
22. S. S. Jacobs, H. H. Helmer, A. Jenkins, *Geophys. Res. Lett.* **23**, 957 (1996); A. M. Smith, *J. Geophys. Res.* **101**, 22749 (1996).
23. The total accumulation volume of the 14 glaciers in the region above the grounding line is 57 km^3/year, derived from the DEM in (*13*), the accumulation data in (*2*), and an ice density of 0.917. Surface ablation over the same area amounts to 16 km^3/year, as calculated from the positive degree-day model [N. Reeh, *Polar Forsch.* **59**, 113 (1991)] and a degree-day factor of 9.8 mm degree^{-1} day^{-1} [T. Konzelmann and R. J. Braithwaite, *J. Glaciol.* **41**, 174 (1995)]. The balance discharge at the grounding line is therefore 41 km^3/year.
24. G. Holdsworth, *J. Glaciol.* **8**, 385 (1969); *Ann. Geophys.* **33**, 133 (1977).
25. A. Weidick, *U.S. Geol. Surv. Prof. Pap. 1386* (Denver, CO, 1995).
26. We thank G. Duchossois, G. Kohlhammer, and the European Space Agency for providing radar data; R. H. Thomas for useful discussions; and C. Werner for providing a synthetic-aperture radar processor. This work was carried out at the Jet Propulsion Laboratory, California Institute of Technology, under a contract with NASA.

16 January 1997; accepted 5 March 1997

Surface Composition of Kuiper Belt Object 1993SC

Robert H. Brown, Dale P. Cruikshank, Yvonne Pendleton, Glenn J. Veeder

The 1.42- to 2.40-micrometer spectrum of Kuiper belt object 1993SC was measured at the Keck Observatory in October 1996. It shows a strongly red continuum reflectance and several prominent infrared absorption features. The strongest absorptions in 1993SC's spectrum occur near 1.62, 1.79, 1.95, 2.20, and 2.32 micrometers in wavelength. Features near the same wavelengths in the spectra of Pluto and Neptune's satellite Triton are due to CH_4 on their surfaces, suggesting the presence of a simple hydrocarbon ice such as CH_4, C_2H_6, C_2H_4, or C_2H_2 on 1993SC. In addition, the red continuum reflectance of 1993SC suggests the presence of more complex hydrocarbons.

Ever since Kuiper (*1*) postulated a remnant population of solar system objects just beyond the orbit of Pluto, there has been speculation as to the existence and nature of these objects, as well as to whether they are representative of the small bodies from which all the known planets are thought to have arisen. Because the Kuiper belt objects (KBOs) were thought to be mostly beyond the range of planetary perturbations, and because they were thought to be too tightly bound to the sun to be perturbed by passing stars, it was hypothesized that KBOs may be primitive remnants of the early solar system (*1*, *2*). In contrast, the Oort cloud, a halo of objects believed to be the source of long-period comets and assumed to extend out to the limits of the sun's gravitational sphere (*3*), may be populated primarily by objects ejected from the region of the giant planets (*4*). Thus, KBOs may not have been as strongly heated as objects populating the Oort cloud and as a result may have unique surface compositional characteristics. KBOs are important to our understanding of the chemistry of the early solar system, but their distance and small size (less than a few hundred kilometers in diameter) precluded discovery until recently. Within the last 4 years, however, over 40 objects have been discovered (*5*). In fact, the Kuiper belt may have $>10^8$ objects larger than 10 km in diameter (*6*).

Detailed here are near-infrared spectroscopic observations of the Kuiper belt object 1993SC, and the implications that these observations have for its surface composition. The observations were conducted at the W. M. Keck Observatory during the period 2 to 4 October 1996 universal time (UT). The Keck I telescope was used with the near-infrared camera (NIRC) as the focal plane instrument. The observations were conducted with the gr120 grism of the NIRC, which has an effective wavelength range in first order of 1.45 to 2.55 μm and a spectral sampling interval of 0.007 μm. The NIRC has an effective pixel size of 0.15 arc sec, and a slit width of 8 pixels (1.2 arc sec) was used for all the spectral observations.

We located 1993SC using the latest orbital elements (*7*) in the commercially available ephemeris program Ephem (*8*) and identified the object in an image taken through the NIRC's K_s filter (*9*). The telescope was then offset 5 arc sec to the north to obtain an additional image and a measurement of the night sky brightness, while tracking the predicted motion of 1993SC. The resulting series of positive-negative pairs in the differenced images showed different apparent position angles, depending on whether or not an object was moving at the sidereal rate. In addition to the position angle difference, objects moving at sidereal rate were trailed. That 1993SC was moving against the stellar background at the predicted rate was corroborated in a final image acquired some 20 min after the initial image, which allowed a check of the total movement of the object against the stellar background.

Collecting a spectrum involved positioning the object in the center of the slit and obtaining pairs of images of 1800 s total exposure (18 separate exposures of 100 s co-added) with each exposure offset along the grism slit by 5 arc sec, alternately north then south. Differencing corresponding pairs of images allowed an accurate subtraction of the sky background

R. H. Brown, Lunar and Planetary Laboratory and Steward Observatory, University of Arizona, Tucson, AZ 85721, USA.
D. P. Cruikshank and Y. Pendleton, NASA Ames Research Center, Moffett Field, CA 94035, USA.
G. J. Veeder, Jet Propulsion Laboratory, California Institute of Technology, Pasadena, CA 91109, USA.

Downloaded from www.sciencemag.org on January 9, 2013

while providing the full time for integration on the object and sky. Our spectrum of 1993SC consists of 3600 s integration over an air-mass range of 1.2 to 1.7.

We corrected telluric extinction by using spectra of several comparison stars obtained on the same night and over the same air-mass range. The spectrum was corrected for the solar color by multiplying the extinction-corrected spectrum by the flux ratio of two blackbodies—one at the color temperature of the comparison star and the other at the color temperature of the sun. The signal-to-noise ratio of the final spectrum was increased at the expense of spectral resolution by convolving the raw spectrum with a 12-channel-wide Gaussian (*10*). This was deemed the best trade-off between increasing the signal-to-noise ratio of the spectrum while reducing spectral resolution (Fig. 1).

There are several apparent absorption bands in the data that are statistically significant. In particular, there is a two-band complex centered near 2.2 and 2.3 μm, respectively, as well as two and perhaps three other significant bands in the 1.4- to 1.9-μm region of the spectrum. The two-band complex near 2.2 and 2.3 μm and the single band near 1.8 μm occur at the same wavelengths as similar features in the spectrum of Triton that are attributed to the presence of CH_4 in solid solution with N_2 ice on Triton's surface (*11*) (Fig. 2). The band structure of the spectra of 1993SC and Triton in the 1.7- to 2.5-μm region are quite similar. The most prominent differences in the two spectra are the greater depths of the bands in the 1993SC spectrum and a mismatch on the short-wavelength side of the band near 1.7 μm. The mismatch on the short-wavelength side of the 1.7-μm band is likely due to the presence of an absorber on 1993SC that is not on Triton. The mismatch in the 1.85-μm region may be due to incomplete extinction correction. In addition to the strong bands, there is an inflection near 2.15 μm in the spectrum of 1993SC that is similar to an inflection in the smoothed Triton spectrum. The inflection in the Triton spectrum is due to N_2 ice (*11*, *12*). Whether the inflection in the spectrum of 1993SC is real and due to N_2 is not clear from these data.

The presence of CH_4 on Triton is based on higher resolution data over a larger wavelength interval (*11*, *12*). At the low resolution of the 1993SC spectrum (and also that of the smoothed Triton spectrum), however, many of the individual bands of CH_4 in this wavelength region cannot be resolved. Nevertheless, the close correspondence of the band centers and widths in the two spectra argues for a light hydrocarbon component on the surface of 1993SC, either CH_4 or a molecule similar in structure and composition such as ethane (C_2H_6), ethylene (C_2H_4), or acetylene (C_2H_2). Ethane, ethylene, and acetylene all have a similar band structure in the 2-μm spectral region because the vibrational modes responsible for the observed bands are similar, producing corresponding similarities in their combination and overtone bands (*13*, *14*). In the 2.5-μm spectral region and at the effective resolution of the 1993SC spectrum, the above molecules are difficult to distinguish spectrally.

Besides the bond structure and the symmetry of a given molecule governing its vibrational spectrum, the electric field environment of a molecule can have important effects on the details of its vibrational spectrum. For example, CH_4 displays shifts to shorter wavelengths in its vibrational bands when it is a minority component in a solid solution with nitrogen (*15*, *16*). This effect led Cruikshank *et al.* (*11*) to conclude that the CH_4 on Triton probably exists in a solid solution with N_2 ice on Triton's surface rather than as free ice in isolated patches. A similar analysis of Pluto's spectrum by Owen *et al.* (*17*) concluded that CH_4 on Pluto also exists in a solid solution with N_2; however, spectra of higher resolution show that the Pluto CH_4 bands are double (*17*), suggesting two reservoirs of CH_4: both free CH_4 and CH_4 dissolved in N_2.

Where CH_4 exists as a solid solution and a free ice, bands centered anywhere between the wavelengths of the bands in each of the end member spectra can be seen at high spectral resolution in a disk-averaged spectrum when the end members are distributed in various proportions as isolated patches on the body's surface (*16*). That is, the spectrum of each of the end members is mixed in proportion to the projected area they occupy on the surface of the body. The effect of reducing the resolution, however, can counteract some or all of this effect, depending on the symmetry of the absorption bands in question. Because the band centers in spectrum of 1993SC are similar to those of Triton, if CH_4 is responsible for most of the absorptions seen in the 1993SC spectrum, then it is tempting to conclude

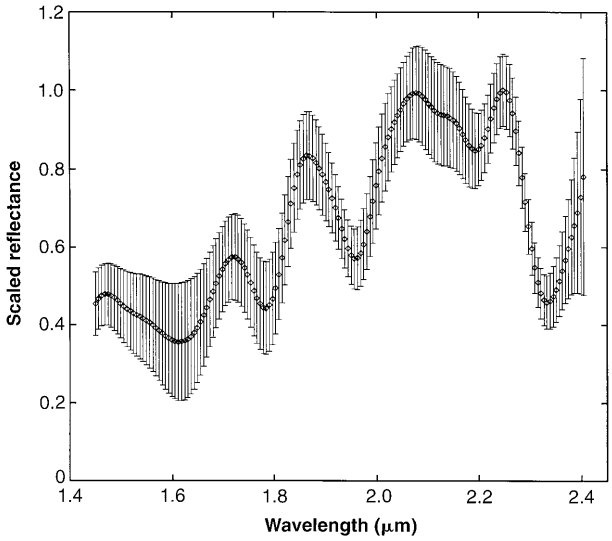

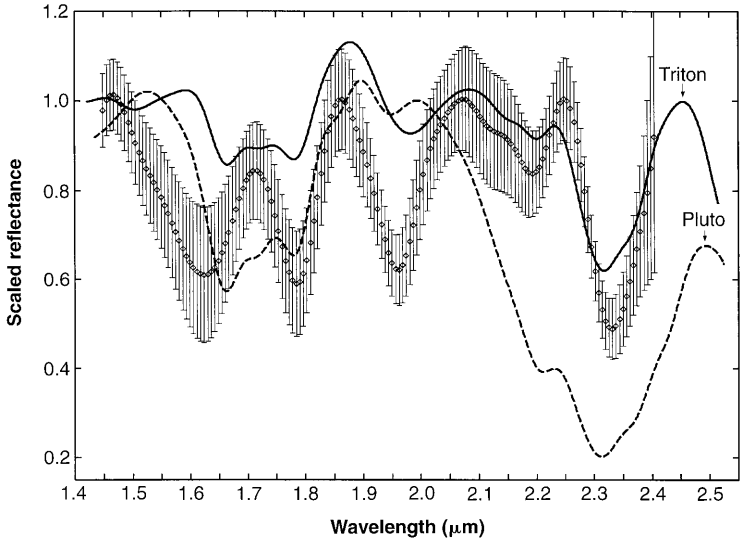

Fig. 1 (**left**). Spectrum of 1993SC. The spectrum has been normalized and convolved with a Gaussian whose full width at half maximum is equal to 12 fundamental resolution elements of the raw spectrum. The error bars are 1σ. **Fig. 2** (**right**). Spectrum of 1993SC plotted with the smoothed spectra of Triton and Pluto. The continuum has been removed from all spectra. The solid line is a spectrum of Triton from Cruikshank *et al.* (*11*), convolved to the same resolution as that of the spectrum of 1993SC. The dotted line is a spectrum of Pluto (*21*), convolved to the resolution of the spectrum of 1993SC. The error bars are 1σ.

Downloaded from www.sciencemag.org on January 9, 2013

that some of the CH_4 on 1993SC exists in a solid solution with another component, perhaps N_2. Nevertheless, the precision and resolution of the existing data combined with the effects cited above make it difficult to reach that conclusion with any certainty.

In addition to the uncertainty introduced when using low-resolution spectral data, it is also unclear whether N_2 on 1993SC could be stable against long-term loss to space. A calculation of the temperature distribution on the surface of a body at a distance of 35 astronomical units from the sun, assuming a bolometric bond albedo of 0.05 and rotation period of 6 hours, gives a peak daytime temperature of 50 K at the equator of a spherical body with very low thermal inertia. At this temperature N_2 and CO have relatively high vapor pressures (4.0 and 0.88 mbar, respectively), but CH_4 ice has a much lower vapor pressure (3 μbar) (*18*). As such, it is unclear whether a body 300 km in diameter (*19*) has enough surface gravity to retain compounds like N_2 and CO over the age of the solar system. Thus, although it is reasonable to conclude that the spectrum of 1993SC is consistent with a CH_4-like hydrocarbon on its surface, making the leap to a CH_4-like hydrocarbon in solid solution with another, more volatile compound like N_2 is thermodynamically problematic.

The spectrum of 1993SC is also interesting because its reflectance increases by about a factor of 2 over the 1.4- to 2.4-μm region. This is much redder than the spectrum of Triton, but slightly less red than the slope of the average visual (0.4 to 0.8 μm) reflectance of 1993SC reported by Luu and Jewitt (*20*). Overall, the spectral slope of 1993SC could be due to complex organic molecules (*21*) on its surface, as well as simple hydrocarbons such as CH_4. Lastly, the similarity of the spectrum of 1993SC to that of Pluto (*22*) (Fig. 2) strengthens the case for CH_4 on 1993SC and appears at least to be consistent with the idea that Pluto and Triton may be the largest members of the population of bodies that made up the early Kuiper belt (*6*). Whether this spectral similarity is significant in light of the possibly very different evolutionary paths taken by Triton, Pluto, and 1993SC is unclear.

REFERENCES AND NOTES

1. G. P. Kuiper, in *Astrophysics: A Topical Symposium*, J. Hynek, Ed. (McGraw-Hill, New York, 1951), pp. 357–424.
2. K. E. Edgeworth, *Mon. Not. R. Astron. Soc.* **109,** 600 (1948)
3. J. H. Oort, *Bull. Astron. Inst. Neth.* **11,** 91 (1950).
4. M. Duncan, T. Quinn, S. Tremaine, *Astrophys. J. Lett.* **328,** L69 (1988).
5. D. Jewitt, J. Luu, J. Chen, *Astron. J.* **112,** 1225 (1996).
6. A. J. Cochran, H. F. Levinson, S. A. Stern, M. J. Duncan, *ibid.* **110,** 342 (1995).
7. Orbital elements were obtained from B. Marsden, Smithsonian Astrophysical Observatory (1996).
8. The program Ephem is marketed by Celestech, P.O. Box 61091, Honolulu, HI 96839, USA.
9. K_s is the K short filter whose passband encompasses the short-wavelength half of the standard K band.
10. The convolution to a lower resolution was done as a pure convolution. The effect of that convolution is to model how the data would look if obtained with an intrinsically lower resolution spectrometer. Application of our convolution technique to other data sets showed that no artifacts were introduced. The effect is simply one of a Fourier filter where the high frequencies in the transform of the data are attenuated by a Gaussian filter.
11. D. P. Cruikshank *et al.*, *Science* **261,** 742 (1993).
12. D. P. Cruikshank, T. C. Owen, C. deBergh, T. Geballe, unpublished data.
13. G. Herzberg, *Infrared and Raman Spectra of Polyatomic Molecules* (Van Nostrand, New York, 1945).
14. R. B. Bohn, S. A. Sandford, L. J. Allamandola, D. P. Cruikshank, *Icarus* **111,** 151 (1994).
15. B. Schmitt, E. Querico, S. Doute, T. Owen, C. deBergh, D. P. Cruikshank, paper presented at the 27th meeting of the Division of Planetary Sciences, American Astronomical Society, Kona, HI, 9 to 13 October 1995.
16. E. Quirico, thesis, Université Joseph Fournier, Grenoble, France (1996).
17. T. C. Owen *et al.*, *Science* **261,** 745 (1993).
18. G. N. Brown and W. T. Zeigler, *Adv. Cryog. Eng.* **25,** 662 (1979).
19. I. P. Williams, D. P. O'Ceallaigh, A. Fitzsimmons, B. G. Marsden, *Icarus* **116,** 180 (1995).
20. J. X. Luu and D. C. Jewitt, *Astron. J.* **111,** 499 (1994).
21. C. Sagan and B. Khare, *Nature* **227,** 102 (1979).
22. T. C. Owen, D. P. Cruikshank, C. deBergh, T. R. Geballe, unpublished data.

23. The W. M. Keck Observatory is operated as a scientific partnership between the California Institute of Technology and the University of California. It was made possible by the generous financial support of the W. M. Keck Foundation. We acknowledge the assistance of W. Harrison at the telescope. We dedicate this paper to the memory of Professor Carl Sagan whose scientific contributions have strongly influenced the concepts presented here.

14 February 1997; accepted 14 April 1997

Modeling of Cometary X-rays Caused by Solar Wind Minor Ions

Roman M. Häberli, Tamas I. Gombosi,* Darren L. De Zeeuw, Michael R. Combi, Kenneth G. Powell

X-ray emission was discovered in comet Hyakutake (C/1996 B2) by the Röntgen satellite in 1996, and these emissions were attributed to the excitation of high charge state solar wind ions due to electron capture from cometary molecules or atoms. Using the plasma flow in the coma of Hyakutake calculated by a three-dimensional adaptive magnetohydrodynamic model, the density distribution of solar wind ions in the coma and the resulting x-ray emission were computed. The calculated High Resolution Imager count rate of 4.4 per second and the spatial distribution of the x-ray emission agree with the observations. A detailed energy spectrum of cometary x-rays is predicted in the 80 to 2000 electronvolt energy range. Cometary x-rays present a sensitive tool to monitor cometary activity and solar wind ion composition.

Observations of comet C/1996 B2 (Hyakutake) by the Röntgen x-ray satellite (ROSAT) revealed the emission of soft x-rays from the coma at an unexpectedly high level of about 10^{25} photons s^{-1} (*1*). Of several possible explanations including fluorescent scattering of solar x-rays, interaction with interplanetary dust particles, and bremsstrahlung created by the cometary plasma, none satisfactorily explains the observed magnitude and shape of the emission (*1*). The observed x-ray emission may be caused by charge exchange excitations (CXE) of high charge state solar wind ions (O^{7+}, O^{6+}, C^{6+}, and others) with neutral molecules or atoms in the comet (*2*). Reactions such as $O^{7+} + H \rightarrow O^{6+*} + H^+$ occur in the upper atmosphere of Jupiter due to interaction with the solar wind, and an analogous mechanism may explain cometary x-rays (*3*). The electron is most likely captured into an excited state of the solar wind minor ion (*4*), leading to emission of soft x-ray and extreme ultraviolet (EUV) radiation. This process is efficient and often used as a diagnostic tool to monitor low-atomic number (Z) elements in laboratory plasmas (*5*).

Using a three-dimensional (3D) single-fluid magnetohydrodynamic (MHD) model of cometary plasma environments (*6*) we calculated the solar wind velocity and streamlines in the coma. The model uses conservation of mass, momentum, and energy, as well as the induction equation to compute the plasma mass density, flow, and pressure and the magnetic field in the coma. Ionization of cometary gas, recombination of ions with electrons and ion-neutral collisions are taken into account as source terms. Adequate resolution in all parts of the coma is ensured by the use of

R. M. Häberli, T. I. Gombosi, D. L. De Zeeuw, M. R. Combi, Space Physics Research Laboratory, University of Michigan, Ann Arbor, MI 48109–2143, USA.
K. G. Powell, Department of Aerospace Engineering, University of Michigan, Ann Arbor, MI 48109–2143, USA.

To whom correspondence should be addressed. E-mail: tamas@umich.edu

Downloaded from www.sciencemag.org on January 9, 2013